5-28-2021

Control of polarization in bulk ferroelectrics by mechanical dislocation imprint

Marion Höfling
Technical University of Darmstadt

Xiandong Zhou
Technical University of Darmstadt

Lukas M. Riemer
École Polytechnique Fédérale de Lausanne

Enrico Bruder
Technical University of Darmstadt

Binzhi Liu
Iowa State University, bzliu@iastate.edu

See next page for additional authors

Control of polarization in bulk ferroelectrics by mechanical dislocation imprint

Abstract

Defects are essential to engineering the properties of functional materials ranging from semiconductors and superconductors to ferroics. Whereas point defects have been widely exploited, dislocations are commonly viewed as problematic for functional materials and not as a microstructural tool. We developed a method for mechanically imprinting dislocation networks that favorably skew the domain structure in bulk ferroelectrics and thereby tame the large switching polarization and make it available for functional harvesting. The resulting microstructure yields a strong mechanical restoring force to revert electric field–induced domain wall displacement on the macroscopic level and high pinning force on the local level. This induces a giant increase of the dielectric and electromechanical response at intermediate electric fields in barium titanate [electric field–dependent permittivity ($\varepsilon 33$) ≈ 5800 and large-signal piezoelectric coefficient ($d33^*$) ≈ 1890 picometers/volt]. Dislocation-based anisotropy delivers a different suite of tools with which to tailor functional materials.

Disciplines

Materials Science and Engineering | Metallurgy

Comments

This is the author's version of the work. It is posted here by permission of the AAAS for personal use, not for redistribution. The definitive version was published in *Science* on May 28, 2021 (vol. 372). DOI: 10.1126/science.abe3810.

Authors

Marion Höfling, Xiandong Zhou, Lukas M. Riemer, Enrico Bruder, Binzhi Liu, Lin Zhou, Pedro B. Groszewicz, Fangping Zhuo, Bai-Xiang Xu, Karsten Durst, Xiaoli Tan, Dragan Damjanovic, Jurij Koruza, and Jürgen Rödel

Control of polarization in bulk ferroelectrics by mechanical dislocation imprint

Marion Höfling[1], Xiandong Zhou[1], Lukas Riemer[3], Enrico Bruder[1], Binzhi Liu[2], Lin Zhou[2,6], Pedro B. Groszewicz[4,5], Fangping Zhuo[1], Bai-Xiang Xu[1], Karsten Durst[1], Xiaoli Tan[2], Dragan Damjanovic[3], Jurij Koruza[1*], Jürgen Rödel[1*]

[1] Department of Materials and Earth Sciences, Technical University of Darmstadt, 64287 Darmstadt, Germany

[2] Department of Materials Science and Engineering, Iowa State University, Ames, IA 50011, USA

[3] Group for Ferroelectrics and Functional Oxides, École Polytechnique Fédérale de Lausanne, 1015 Lausanne, Switzerland

[4] Institute of Physical Chemistry, Technical University of Darmstadt, 64287 Darmstadt, Germany

[5] Present address: Department of Radiation Science and Technology, Delft University of Technology, Delft 2629JB, Netherlands

[6] Ames Laboratory, U.S.-DOE, Ames, IA 50011, USA

*Correspondence to: koruza@ceramics.tu-darmstadt.de, roedel@ceramics.tu-darmstadt.de

Abstract:

Defects are essential to engineer properties of functional materials, ranging from semiconductors and superconductors to ferroics. While point defects have been widely exploited, dislocations are commonly viewed as problematic for functional materials and not as a microstructural tool. We developed a method for mechanically imprinting dislocation networks which favorably skew the domain structure in bulk ferroelectrics and thereby tame the large switching polarization and make it available for functional harvesting. The resulting microstructure yields a strong mechanical restoring force to revert electric field-induced domain wall displacement on the macroscopic level and high pinning force on the local level. This induces a giant increase of the dielectric and electromechanical response at intermediate electric fields in Barium Titanate (ε_{33}≈5800 and d_{33}*≈1890 pm/V). Dislocation-based anisotropy delivers a different suite of tools to tailor functional materials.

One Sentence Summary:

Mechanical dislocation imprint establishes a macroscopic restoring force which allows to tame and harvest giant switching from ground state.

Main Text:

Ferroelectricity, like ferromagnetism and superconductivity, belongs to the class of cooperative phenomena. Strain engineering allows us to drastically impact related properties of thin films with a judicious choice of substrate materials. Strain engineering has been demonstrated for the cases of ferromagnetic materials (*1*) and superconductors (*2*). For ferroelectric films, phase transition temperatures have been enhanced by 400 °C (*3*) and even non-ferroelectric materials have been made ferroelectric (*4*). Introducing dislocations allows localized strain engineering and affects the polarization reversal process (*5*). While dislocations are generally the culprits for degraded performance in functional oxides that are usually avoided at all costs, some excellent examples exist that demonstrate their utility. Dislocations enable strong vortex pinning in high-temperature superconductors (*6*) required for high critical currents, while in thermoelectrics they increase the heat-to-electricity conversion efficiency by affecting phonon scattering (*7*). In oxides, dislocations are not only associated with the surrounding strain fields, but often also exhibit charged cores and screening space-charge layers (*8*). These peculiar mechanical and electrical characteristics offer a large, yet mostly unexplored, potential to alter not only thermal (*7*), but also electrical conductivity (*8, 9*). Numerical simulations also confirmed the potential for interaction of dislocations with fundamental order parameters, such as spontaneous polarization (P_s) and strain (*10, 11*).

Obtaining high intrinsic electromechanical response and manipulating the mobility of ferroelectric domain walls (labelled as extrinsic contribution (*12*)) are two key challenges that exist in bulk ferroelectrics. Some common approaches for increasing the ferroelectric properties are strain engineering (*4*), polarization rotation (*13*), construction of phase boundaries (*14*), and exploitation of critical points (*15*). State-of-the-art concepts to control domain wall motion include point defect doping (*16, 17*), domain engineering (*18, 19*), and texturing (*20*).

We developed a method that utilizes dislocations to interact with the fundamental order and field parameters of bulk ferroelectric oxides, i.e., polarization and strain, at different length scales. This directly impacts the force on and thereby the movement of domain walls. It introduces a temperature-stable macroscopic restoring force acting against the applied electric field, allows us to tune the dielectric and electromechanical properties. We term our process mechanical dislocation imprinting because it is reminiscent of mechanical imprinting used for engraving names or security codes. We also distinguish our process from one where an electric charge is imprinted (*21, 22*).

We used mechanical creep to introduce a directional dislocation network into ⟨001⟩-oriented $BaTiO_3$ single crystals (Fig. S1) and demonstrated that the dislocations act as nucleation sites for ferroelectric domain walls. The mechanical dislocation imprint causes a 19-fold increase in the large-signal piezoelectric coefficient, d_{33}^*. Our methodology is readily accessible for furnishing bulk functional materials with permanent, tailored anisotropy.

The mechanical imprint is macroscopically reflected in the changed domain structure. The original lamellar domain configuration (*23*) (Fig. 1A) was changed into an unconventional rhombic domain structure with both clear and cloudy regions after high-temperature deformation (Fig. 1B, C, D). Both regions exhibit a multi-domain state with different domain density (Fig. S2). The plastic deformation enforces an anisotropy with 2/3rds of the domains in the deformed sample aligned along the deformation axis [001] (Fig. S3). We used Electron Channeling Contrast Imaging (ECCI, Fig. S4) to provide a microscopic view, featuring the orientation of

imprinted glide planes on the surface. The dislocation spacing is in the range 80–450 nm (Fig. S4C). We used controlled indentation (Fig. S4D) as benchmark for observed dislocation structures. We used Transmission Electron Microscopy (TEM, Fig. S5) to reveal a Burgers vector of $\boldsymbol{b}=a[101]$, a being the lattice parameter. ECCI and TEM images confirm for us the successful dislocation imprint by activation of the $\{101\}\langle 101\rangle$ slip system.

Dislocations are associated with high local tensile and compressive stress fields (Fig. S6A, B) and, in some oxides, with a charged dislocation core. In ferroelectrics, this prompts a nucleation of domain walls (*24*). In our samples this results in a rhombic domain structure (Fig. 1B, D). We investigated the influence of the dislocations on the domain structure and the switching behavior using mechanically-coupled Phase-Field (PF) simulations based on Ginzburg-Landau equations. The P_2 polarization component for a stable equilibrium configuration without dislocations is depicted in Fig. 2A, whereby straight 90° domain walls were formed on the {101} plane. We simulated the active slip system (Fig. 2B) with 8 edge dislocations (Burgers vector $|\boldsymbol{b}|$=0.56 nm) forming a dislocation array with $\boldsymbol{b}=a[101]$. From these results, we determined that the domain wall becomes kinked and broadens in the vicinity of a dislocation. Fluctuations of the local polarization and stress were strongly increased (Fig. 2B, Fig. S6A, B). This increase is in agreement with previous simulations investigating the impact of dislocation spacing, h, Burgers vector, and the strength of the dislocation-domain interaction (*10, 11*) on the fluctuation of the local polarization.

We found a domain wall pinning effect of the dislocations using temperature-dependent in-situ TEM, resulting in a controlled and localized nucleation and motion of the domain walls (Fig. 2C; Movie S1). A similar effect had been predicted by simulations (*25*) and was reported in $Pb(Zr,Ti)O_3$ thin films with field-dependent in-situ TEM (*26*). Upon cooling through the Curie temperature (120 °C), T_c, the first domain nucleated at the lower dislocation segment (I, dark arrow in Fig. 2C, c_1) and grew until it reached the upper dislocation segment. The latter pinned the domain temporarily (Fig. 2D) before it could overcome the dislocation barrier upon further cooling (Fig. 2C, c_4). In the meantime two new domains (II, III) nucleated at the lower dislocation segment. At room temperature (Fig. 2C, c_4) domain I was blocked by a {101} domain wall, while domains II and III were still blocked by the upper dislocation segment. The dislocation-domain wall interactions we observed in the TEM were corroborated by PF simulations as function of electric field and temperature (Fig. S7A, B).

Macroscopically, the increase in population density of c-domains (out-of-plane P_s) versus a-domains (in-plane P_s) in the unpoled sample (Fig. S3) caused reduction of the permittivity after deformation (Fig. S8A) due to anisotropy of the dielectric tensor of BT with $\varepsilon_a > \varepsilon_c$. In contrast, the poled deformed samples retained a high fraction of a-domains (Fig. S3), leading to an enhanced permittivity (by a factor of five) as compared to the reference samples. Clearly, domain wall density will also come into play (*18*), but this appears to be a secondary issue.

Application of large-signal super-coercive fields (Fig. 3A) highlights the drastic impact of mechanical dislocation imprint. Despite loop saturation, polarization does not reach the expected spontaneous polarization value of 26 µC/cm², indicating domain wall pinning. Concurrently, we observed a four-fold increase in domain back-switching ($P_{back}=P_{max}{}^*-P_{rem}{}^*$) as compared to reference undeformed samples (Fig. S9), which indicates a strong macroscopic restoring force. The apparent coercive field, $E_c{}^*$ is strongly enhanced, supporting domain wall pinning (for statistical confirmation, see Fig. S9).

The full potential of the dislocation-domain wall interaction was obtained in the intermediate E-field regime (below E_c*). Increasing the amplitude of the applied AC electric field beyond the small-signal excitation resulted in stronger domain wall vibration, while the restoring force imposed by the presence of *a*-domains tuned this displacement and ensured a back-switching of domains in regions with high dislocation density. As a result, both the large-signal dielectric permittivity and the piezoelectric coefficient increased exponentially at approximately E/E_c*= *0.1* and reached ε_r'≈5810 and d_{33}*≈1890 pm/V at E/E_c*=*0.17*, respectively (Fig. 3B). The d_{33}* value was about 19 times higher as compared to the undeformed reference sample (d_{33}*≈98 pm/V, ε_r'≈170). Due to the long-range restoring force, this domain wall motion was almost anhysteretic below E_c* (Fig. S10). Note that the high permittivity and piezoelectric coefficient values remained stable up to 130,000 AC cycles (Fig. S11) and a temperature of 75 °C (Fig. S12 A,B). In addition, the overall behavior features a weak frequency dependence in d_{33}*(Fig. S13).

Our results indicate that the uniaxial stress activates four out of six available glide planes. Ensuing dislocation networks stabilize two domain wall variants (a_1-*c* and a_2-*c*) but disfavor the a_1-a_2 variant (Fig. S3). Thereby the imprinted mechanical dislocation structure causes an anisotropy in the domain structure, both in the unpoled and the poled state. The enforced presence of the *a*-domains provides a strain incompatibility to electric field-enforced *c*-domains resulting in an elastic macroscopic restoring force akin to the case of thin films where the strain incompatibility is provided by the substrate. Locally, the dislocation network sitting on exactly the same plane as the domain wall provides a pinning force. The latter is confirmed by our numerical model (Fig. 3C) demonstrating pinning of a domain wall at a single dislocation. Domain wall bending and reversible domain wall movement increase up to $E=E_{pin}$. Above E_{pin} the domain wall overcomes the local pinning potential. At the pinning electric field, glide planes with low dislocation density become locally unpinned in an irreversible manner but the overall remaining strain incompatibility ensured by glide planes with high dislocation density stabilizes the *a*-*c* domain wall variant (Fig. 3D and Fig. S14) and ensures complete back-switching (Fig. S15). We visualized the increased density of *a*-*c* domain walls after deformation in the unpoled and poled state (Fig. 3E). We observed that mechanical dislocation imprint maintains a thermally-stable piezoelectric coefficient up to 75 °C. In a $SrTiO_3$ perovskite,-dislocation structures have been reported to feature stability up to 600 °C (*8*) offering pinning sites in a large temperature range. Similar reversal to the domain structure at zero electric field can only be enforced by external mechanical compressive stress (*27*). Current material design options include utilization of point defects (*17*) or complex poling conditions stabilizing independently *a*-domains and *c*-domains in different sample volumes (*19*). These design options are until now not used for practical purposes as they are stable only for a limited number of electrical cycles and at low temperatures (*19*) or limited electric field levels (*20*). Our dislocation-based mechanism is fundamentally different from acceptor doping (*17*), where pinning centers are homogeneously distributed allowing only relatively short motion of domain walls. In mechanically deformed samples dislocations are concentrated in some parts of the sample and depinned domain walls can therefore move for longer distances. In bulk ceramics, templated grain growth (*28*, *29)* affords outstanding properties, as demonstrated for energy storage materials with supreme reliability *(30)*.

Mechanical dislocation imprint provides a powerful mechanism to extend the local pinning potential of dislocations to the macroscopic level of bulk ceramics. Whereas in thin films the substrate provides the tool for strain engineering and misfit dislocations are indispensable (*31*), in bulk materials dislocations have to be introduced via creep, plastic deformation or novel

methods like flash sintering (*32*). Uniaxial stress selects a specific dislocation structure which installs the in-plane strain permanently into the volume thus providing a macroscopic restoring force. In addition, this method avails a dislocation structure for local effects like domain wall pinning. This mechanical dislocation imprint ~~walls~~ both tames strong domain wall switching under applied electric field and allows to harvest this strain change due to mechanically enforced back-switching. Subcoercive electric fields ~~to~~ therefore reach extraordinary piezoelectric coefficients. This mechanism extends the available spectrum of tools for designing the functional properties of bulk functional materials such as ferroics and superconductors.

References:

1. R. S. Beach, J. A. Borchers, A. Matheny, R. W. Erwin, M. B. Salamon, B. Everitt, K. Pettit, J. J. Rhyne, C. P. Flynn, Enhanced curie temperatures and magnetoelastic domains in Dy/Lu superlattices and films. *Phys. Rev. Lett.* **70**, 3502-3505 (1993).
2. I. Bozovic, G. Logvenov, I. Belca, B. Narimbetov, I. Sveklo, Epitaxial strain and superconductivity in $La_{2-x}Sr_xCuO_4$ thin films. *Phys. Rev. Lett.* **89**, 4 (2002).
3. K. J. Choi, M. Biegalski, Y. L. Li, A. Sharan, J. Schubert, R. Uecker, P. Reiche, Y. B. Chen, X. Q. Pan, V. Gopalan, L. Q. Chen, D. G. Schlom, C. B. Eom, Enhancement of ferroelectricity in strained $BaTiO_3$ thin films. *Science* **306**, 1005-1009 (2004).
4. J. H. Haeni, P. Irvin, W. Chang, R. Uecker, P. Reiche, Y. L. Li, S. Choudhury, W. Tian, M. E. Hawley, B. Craigo, A. K. Tagantsev, X. Q. Pan, S. K. Streiffer, L. Q. Chen, S. W. Kirchoefer, J. Levy, D. G. Schlom, Room-temperature ferroelectricity in strained $SrTiO_3$. *Nature* **430**, 758-761 (2004).
5. S. V. Kalinin, B. J. Rodriguez, A. Y. Borisevich, A. P. Baddorf, N. Balke, H. J. Chang, L. Q. Chen, S. Choudhury, S. Jesse, P. Maksymovych, M. P. Nikiforov, S. J. Pennycook, Defect-mediated polarization switching in ferroelectrics and related materials: From mesoscopic mechanisms to atomistic control. *Adv. Mater.* **22**, 314-322 (2010).
6. B. Dam, J. M. Huijbregtse, F. C. Klaassen, R. C. F. van der Geest, G. Doornbos, J. H. Rector, A. M. Testa, S. Freisem, J. C. Martinez, B. Stauble-Pumpin, R. Griessen, Origin of high critical currents in $YBa_2Cu_3O_7$-delta superconducting thin films. *Nature* **399**, 439-442 (1999).
7. S. I. Kim, K. H. Lee, H. A. Mun, H. S. Kim, S. W. Hwang, J. W. Roh, D. J. Yang, W. H. Shin, X. S. Li, Y. H. Lee, Dense dislocation arrays embedded in grain boundaries for high-performance bulk thermoelectrics. *Science* **348**, 109-114 (2015).
8. K. K. Adepalli, J. Yang, J. Maier, H. L. Tuller, B. Yildiz, Tunable oxygen diffusion and electronic conduction in $SrTiO_3$ by dislocation-induced space charge fields. *Adv. Funct. Mater.* **27**, 1700243 (1700241-1700249) (2017).
9. L. Porz, T. Frömling, A. Nakamura, N. Li, R. Maruyama, K. Matsunaga, P. Gao, H. Simons, C. Dietz, M. Rohnke, J. Janek, J. Rödel, Conceptual framework for dislocation-modified conductivity in oxide ceramics deconvoluting mesoscopic structure, core, and space charge exemplified for $SrTiO_3$. *ACS Nano* **in print**, (2020).
10. A. Kontsos, C. M. Landis, Computational modeling of domain wall interactions with dislocations in ferroelectric crystals. *Int. J. Solids Struct.* **46**, 1491-1498 (2009).
11. H. H. Wu, J. Wang, S. G. Cao, T. Y. Zhang, Effect of dislocation walls on the polarization switching of a ferroelectric single crystal. *Appl. Phys. Lett.* **102**, 232904 (2013).
12. D. Damjanovic, Ferroelectric, dielectric and piezoelectric properties of ferroelectric thin films and ceramics. *Rep. Prog. Phys.* **61**, 1267-1324 (1998).
13. H. X. Fu, R. E. Cohen, Polarization rotation mechanism for ultrahigh electromechanical response in single-crystal piezoelectrics. *Nature* **403**, 281-283 (2000).
14. R. Guo, L. E. Cross, S. E. Park, B. Noheda, D. E. Cox, G. Shirane, Origin of the high piezoelectric response in $PbZr_{1-x}Ti_xO_3$. *Phys. Rev. Lett.* **84**, 5423-5426 (2000).
15. Z. Kutnjak, J. Petzelt, R. Blinc, The giant electromechanical response in ferroelectric relaxors as a critical phenomenon. *Nature* **441**, 956-959 (2006).
16. K. Carl, K. H. Härdtl, Electrical aftereffects in pb(ti,zr)o_3 ceramics. *Ferroelectrics* **17**, 473-486 (1978).
17. X. B. Ren, Large electric-field-induced strain in ferroelectric crystals by point-defect-mediated reversible domain switching. *Nat. Mater.* **3**, 91-94 (2004).
18. S. Wada, T. Muraishi, K. Yokoh, K. Yako, H. Kamemoto, T. Tsurumi, Domain wall engineering in lead-free piezoelectric crystals. *Ferroelectrics* **355**, 37-49 (2007).
19. Q. Wang, F. Li, Large actuation strain over 0.3% in periodically orthogonal poled batio$_3$ ceramics and multilayer actuators via reversible domain switching. *J. Phys. D Appl. Phys.* **51**, 255301 (2018).
20. Y. Saito, H. Takao, T. Tani, T. Nonoyama, K. Takatori, T. Homma, T. Nagaya, M. Nakamura, Lead-free piezoceramics. *Nature* **432**, 84-87 (2004).
21. N. Hur, S. Park, P. A. Sharma, J. S. Ahn, S. Guha, S. W. Cheong, Electric polarization reversal and memory in a multiferroic material induced by magnetic fields. *Nature* **429**, 392-395 (2004).
22. B. Akkopru-Akgun, W. Zhu, M. T. Lanagan, S. Trolier-McKinstry, The effect of imprint on remanent piezoelectric properties and ferroelectric aging of $PbZr_{0.52}Ti_{0.48}O_3$ thin films. *J. Am. Ceram. Soc.* **102**, 5328-5341 (2019).

23. W. J. Merz, Domain properties in $BaTiO_3$. *Phys. Rev.* **88**, 421-422 (1952).
24. R. C. Bradt, G. S. Ansell, Dislocations and 90 degrees domains in barium titanate. *J. Appl. Phys.* **38**, 5407-5408 (1967).
25. S. Y. Hu, Y. L. Li, L. Q. Chen, Effect of interfacial dislocations on ferroelectric phase stability and domain morphology in a thin film - a phase-field model. *J. Appl. Phys.* **94**, 2542-2547 (2003).
26. P. Gao, C. T. Nelson, J. R. Jokisaari, S. H. Baek, C. W. Bark, Y. Zhang, E. G. Wang, D. G. Schlom, C. B. Eom, X. Q. Pan, Revealing the role of defects in ferroelectric switching with atomic resolution. *Nat. Commun.* **2**, 1-6 (2011).
27. E. Burcsu, G. Ravichandran, K. Bhattacharya, Large strain electrostrictive actuation in barium titanate. *Appl. Phys. Lett.* **77**, 1698-1700 (2000).
28. G. L. Messing, S. Poterala, Y. Chang, T. Frueh, E. R. Kupp, B. H. Watson, R. L. Walton, M. J. Brova, A.-K. Hofer, R. Bermejo, R. J. Meyer, Texture-engineered ceramics–property enhancements through crystallographic tailoring. *J. Mater. Res.* **32**, 3219-3241 (2017).
29. S. Kong, J. Daniels, Grain-scale strain heterogeneity as a function of crystallographic texture in phase-change electro-mechanical ceramics. *Appl. Phys. Lett.* **117**, (2020).
30. J. Li, Z. Shen, X. Chen, S. Yang, W. Zhou, M. Wang, L. Wang, Q. Kou, Y. Liu, Q. Li, Z. Xu, Y. Chang, S. Zhang, F. Li, Grain orientation engineered multilayer ceramic capacitors for energy storage applications. *Nat. Mater.* **19**, 999–1005 (2020).
31. M. W. Chu, I. Szafraniak, R. Scholz, C. Harnagea, D. Hesse, M. Alexe, U. Gosele, Impact of misfit dislocations on the polarization instability of epitaxial nanostructured ferroelectric perovskites. *Nat. Mater.* **3**, 87-90 (2004).
32. J. Cho, J. Li, H. Wang, Q. Li, Z. Fan, A. K. Mukherjee, W. Rheinheimer, H. Wang, X. Zhang, Study of deformation mechanisms in flash-sintered yttria-stabilized zirconia by in-situ micromechanical testing at elevated temperatures. *Mater. Res. Lett.* **7**, 194-202 (2019).
33. S. Beauchesne, J. P. Poirier, Creep of barium titanate perovskite: A contribution to a systematic approach to the viscosity of the lower mantle. *Phys. Earth Planet. Inter.* **55**, 187-199 (1989).
34. J.-P. Poirier, *Creep of crystals: High-temperature deformation processes in metals, ceramics and minerals*. Cambridge earth science series (Cambridge University Press, Cambridge, 1985).
35. N. Doukhan, J. C. Doukhan, Dislocations in perovskites $BaTiO_3$ and $CaTiO_3$. *Phys. Chem. Minerals* **13**, 403-410 (1986).
36. S. Taeri, D. Brunner, W. Sigle, M. Rühle, Deformation behaviour of strontium titanate between room temperature and 1800 k under ambient pressure. *Z. Metallk.* **95**, 433-446 (2004).
37. W. Blum, P. Eisenlohr, F. Breutinger, Understanding creep - a review. *Metall. Mater. Trans. A* **33**, 291-303 (2002).
38. D. Berlincourt, H. Jaffe, Elastic and piezoelectric coefficients of single crystal barium titanate. *Phys. Rev.* **111**, 143-148 (1958).
39. M. I. Morozov, D. Damjanovic, Charge migration in $Pb(Zr,Ti)O_3$ ceramics and its relation to ageing, hardening, and softening. *J. Appl. Phys.* **107**, 034106 (2010).
40. S. Zaefferer, N.-N. Elhami, Theory and application of electron channelling contrast imaging under controlled diffraction conditions. *Acta Mater.* **75**, 20-50 (2014).
41. Y. L. Li, S. Y. Hu, S. Choudhury, M. I. Baskes, A. Saxena, T. Lookman, Q. X. Jia, D. G. Schlom, L. Q. Chen, Influence of interfacial dislocations on hysteresis loops of ferroelectric films. *J. Appl. Phys.* **104**, 104110 (2008).
42. Y. L. Li, L. E. Cross, L. Q. Chen, A phenomenological thermodynamic potential for $BaTiO_3$ single crystals. *J. Appl. Phys.* **98**, (2005).
43. W. Cai, A. Arsenlis, C. R. Weinberger, V. V. Bulatov, A non-singular continuum theory of dislocations. *J. Mech. Phys. Solids* **54**, 561-587 (2006).
44. S. P. Alpay, I. B. Misirlioglu, V. Nagarajan, R. Ramesh, Can interface dislocations degrade ferroelectric properties? *Appl. Phys. Lett.* **85**, 2044-2046 (2004).
45. B. X. Xu, D. Schrade, R. Muller, D. Gross, T. Granzow, J. Rodel, Phase field simulation and experimental investigation of the electro-mechanical behavior of ferroelectrics. *Zamm-Z. Angew. Math. Me.* **90**, 623-632 (2010).
46. S. Wang, M. Yi, B. X. Xu, A phase-field model of relaxor ferroelectrics based on random field theory. *Int. J. Solids Struct.* **83**, 142-153 (2016).

47. C. J. Permann, D. R. Gaston, D. Andrš, R. W. Carlsen, F. Kong, A. D. Lindsay, J. M. Miller, J. W. Peterson, A. E. Slaughter, R. H. Stogner, R. C. Martineau, Moose: Enabling massively parallel multiphysics simulation. *SoftwareX* **11**, 100430 (2020).
48. W. J. Merz, The electric and optical behavior of $BaTiO_3$ single-domain crystals. *Phys. Rev.* **76**, 1221-1225 (1949).
49. G. A. Schneider, T. Scholz, J. Muñoz-Saldana, M. V. Swain, Domain rearrangement during nanoindentation in single-crystalline barium titanate measured by atomic force microscopy and piezoresponse force microscopy. *Appl. Phys. Lett.* **86**, 3 (2005).
50. F. Javaid, K. E. Johanns, E. A. Patterson, K. Durst, Temperature dependence of indentation size effect, dislocation pile-ups, and lattice friction in (001) strontium titanate. *J. Am. Ceram. Soc* **101**, 356-364 (2018).

Acknowledgments:

Authors would like to thank Sophie Bauer and Kuan Ding for providing the reference indent in $BaTiO_3$, Jonas Lins for the acquisition of the NMR spectra and Gerd Buntkowsky for the access to the NMR spectrometer. BX und XZ thank for the access to the Lichtenberg High-Performance Computer and the technical support from the HHLR, Technical University of Darmstadt.

Funding: This work is supported by the project No. 414179371 of the German Research Foundation (DFG). The TEM experiments, performed at the Sensitive Instrument Facility at Ames Laboratory, were supported by the USA National Science Foundation (NSF), through grant No. DMR-1700014. LR acknowledges the financial support from the Swiss National Science Foundation (grant No 200021 172525). PG and JK acknowledge the support of the Profile Area "PMP" of TU Darmstadt for providing the goniometer NMR probe. The phase-field simulation work is partially funded by the project No. 398072825 of German Research Foundation (DFG).

Author contributions: MH prepared the samples. MH and LR performed the dielectric and electromechanical measurements while FZ provided confirmation on an independent orientation. JR and JK designed the experiments and supervised together with DD the analysis of the data. XZ and BX performed the phase field simulations. BL, LZ and XT carried out the TEM analysis. PG planned and analyzed the NMR measurements and EB the ECCI measurements. DD, JR, JK, MH and KD discussed the deformation mechanisms. MH, JK and JR prepared the manuscript and all authors contributed and commented on the text.

Competing interests: Authors declare no competing interests.

Data and materials availability: All data is available in the main text or the supplementary materials

Supplementary Materials:

Materials and Methods

Supplementary Text

Figures S1-S15

Movie S1

References (*33-50*)

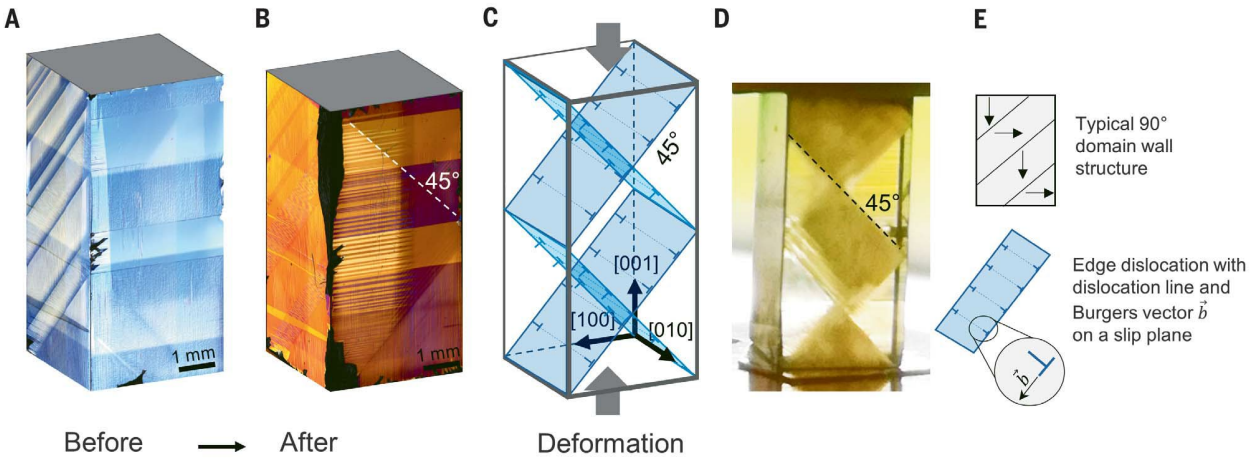

Fig. 1. Changes of the ferroelectric domain configuration by mechanical dislocation imprint. (**A**) Typical domain arrangement for a tetragonal ⟨001⟩-oriented undeformed $BaTiO_3$ single crystal (*23*), imaged with differential interference contrast (DIC), causing the change in colour. Same imaging method is applied in (**B)** for the deformed sample. (**C**) The schematic presentation of the set of slip systems {101}⟨101⟩ activated during uniaxial deformation at high temperature. This introduces a directional dislocation network resulting in a reorientation of the domains according to the slip planes highlighted in (**C**), yielding a highly unusual rhombic domain structure in (**D**) (photography).Both, cloudy and clear regions in (**B**) and (**D**) exhibit a multi-domain state with different domain density (Fig. S2). (**E**) Schematic of the typical 90° domain alignment and the dislocations with dislocation line and Burgers vector.

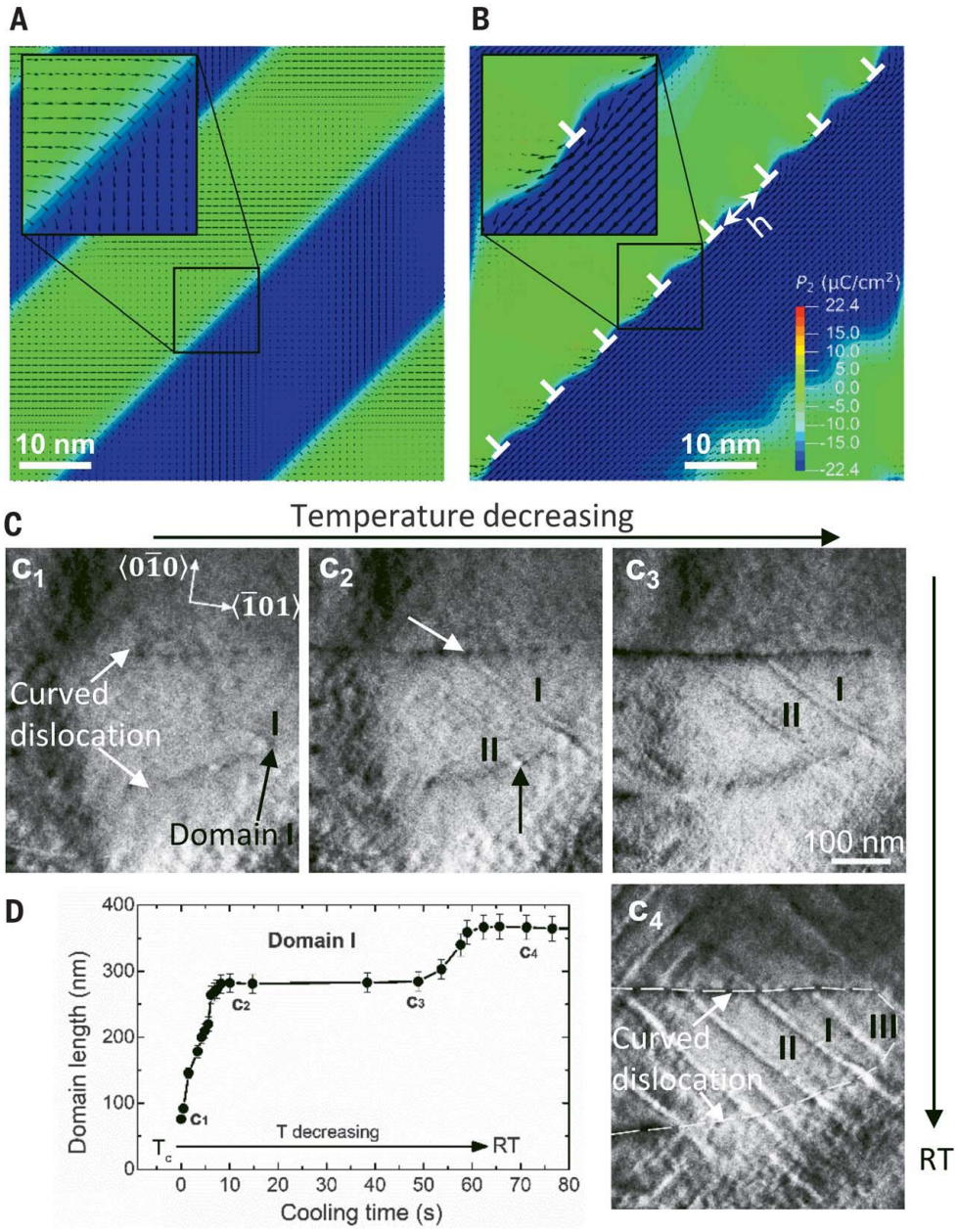

Fig. 2. Influence of dislocations on domain nucleation and mobility. The steady state of local polarization without (**A**) and with (**B**) 8 edge dislocations, along the {101} plane is studied by phase-field simulations. Dislocations lead to both wavy domain walls and fluctuation of polarization amplitude, as demonstrated by the inset of (**B**). (**C**) In-situ TEM study on a curved dislocation line during cooling through T_c (see Movie S1). Domain I nucleates at the lower segment of the dislocation (dark arrow in **c**$_1$), grows until it reaches the upper dislocation segment (white arrow in **c**$_2$) and is there pinned for a period of 40 s (**D**). Domains II (black arrow in **c**$_2$) and III are formed at the lower dislocation segment and grow until RT is reached (**c**$_4$). The temperature decrease is indicated with black arrows along the TEM images. Here, we present the link between simulated domain nucleation at the dislocation (**B**) and the formation of domains at the dislocation in temperature-dependent in-situ TEM.

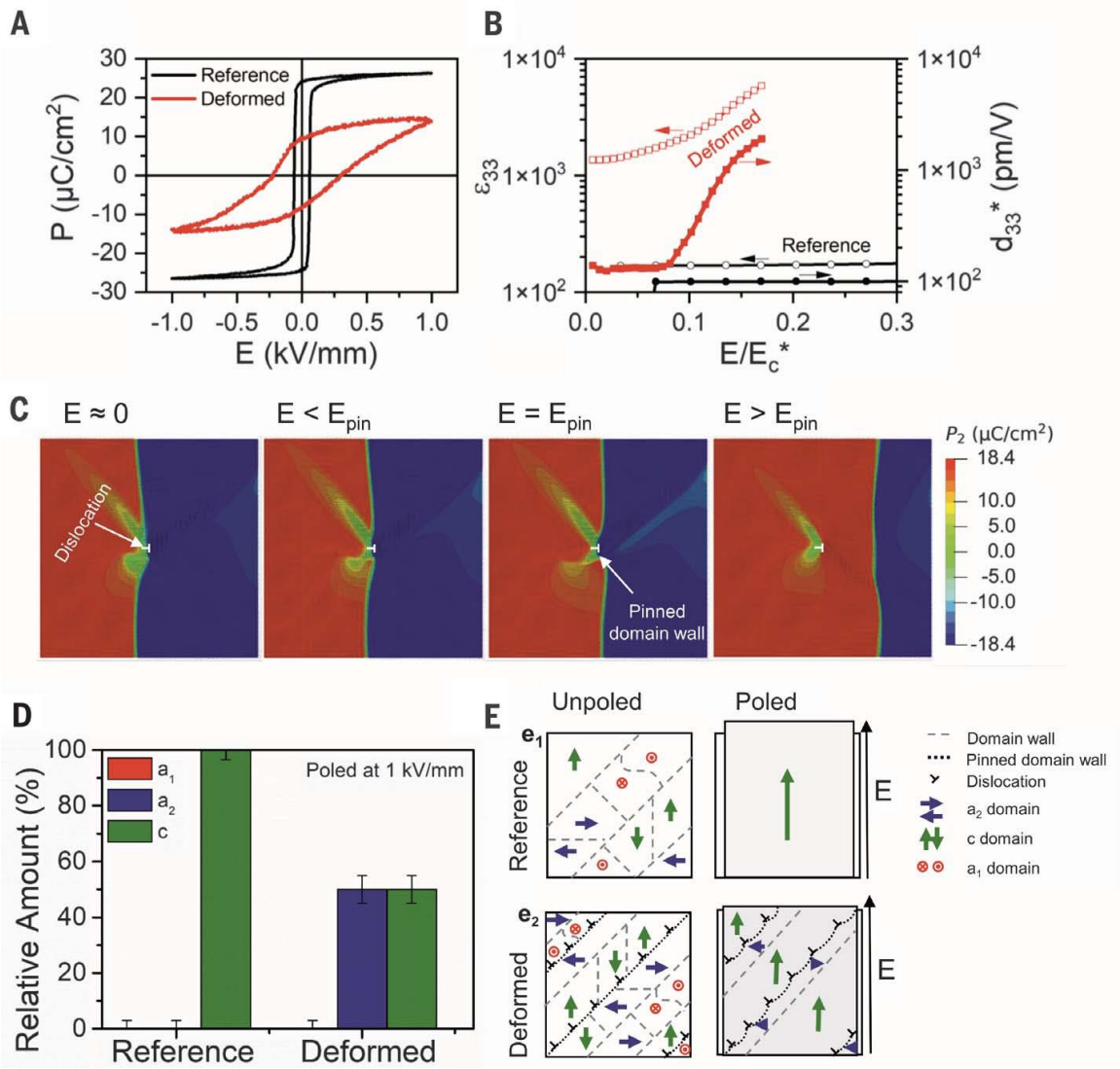

Fig. 3. Influence of mechanical dislocation imprint on electrical properties. A, Presence of dislocations yields a decrease in P_{max}^* and pronounced back-switching. (**B**) Substantial increase in d_{33}^* and ε_{33} for the poled deformed sample with increasing AC electric field (normalized by E_c^* - apparent coercive field at 1 kV/mm). (**C**) Simulation of domain wall-dislocation interaction; when the electric field is relatively low the domain wall is pinned at the dislocation, gets kinked and bent. When a pinning electric field is reached, the wall can break through the barrier of a single dislocation. (**D**) Comparison of the domain distribution of a reference and a deformed sample poled at 1 kV/mm, as obtained from NMR measurements (Fig. S3). The domain structures are schematically depicted in (**E**). Due to pinning of the *a*-*c* domain-walls at the dislocation and the resulting macroscopic restoring force, the total net expansion in the *c* direction is reduced, as compared to the undeformed reference sample, but the switchable strain is strongly enhanced.